Sources of Sahel Precipitation for Simulated Drought and Rainy Seasons

LEONARD M. DRUYAN

NASA Goddard Space Flight Center, Institute for Space Studies, New York.

RANDAL D. KOSTER

NASA Goddard Space Flight Center, Greenbelt, Maryland.

(Manuscript received 1 December 1988, in final form 22 June 1989)

ABSTRACT

The sources of sub-Saharan precipitation are studied using diagnostic procedures integrated into the code of the GISS climate model. Water vapor evaporating from defined source regions is "tagged," allowing the determination of the relative contributions of each evaporative source to the simulated July rainfall in the Sahel. Two June–July simulations are studied to compare the moisture sources, moisture convergence patterns and the spatial variations of precipitation for rainy and drought conditions. Results for this case study indicate that patterns of moisture convergence and divergence over northern Africa had a stronger influence on model rainfall over the sub-Sahara than did evaporation rates over the adjacent oceans or moisture advection from ocean to continent. While local continental evaporation contributed significant amounts of water to Sahelian precipitation in the "rainy" simulation, moisture from the Indian Ocean did not precipitate over the Sahel in either case.

1. Introduction

The Sahel, a swath across Africa located between 10° and 20°N, is a semiarid region that is at the northern fringe of summer monsoon rains. These rains have been so sparse during the past 20 years, compared with the earlier part of this century, that the literature has referred to a persistent Sahelian drought.

The moisture supply for Sahel summer rains is discerned in the analysis of the water vapor transports associated with 1979 summer rains by Cadet and Nnoli (1987). A large maximum in the northward moisture flux over the eastern South Atlantic Ocean extends across the equator and covers the Gulf of Guinea by late spring, continuing into the summer. Moreover, the analyses indicate that north of about 10°N low-level moisture is advected from the Atlantic Ocean eastward over the Sahel in ever increasing fluxes between late spring and summer. While there was some evidence that reduced northward moisture fluxes, penetrating 12°N during July, resulted in decreases in precipitation by August, there was no opportunity to compare the water vapor budget of a drought season with a rainy one since the study was confined to 1979.

Lamb (1983) did compare the strength of water vapor fluxes over West Africa during three Sahel drought years and three seasons of near-normal rainfall. He concluded that

> Subsaharan drought is probably not (and certainly not necessarily) associated with the northward supply of unusually dry surface air to West Africa from the tropical Atlantic.

This conclusion was based on an analysis of the atmospheric moisture content of air along the Gulf of Guinea coast during each of the summers. On the other hand, he also found that the southwesterly flow of moist monsoon air was generally thinner at 13°N over West Africa for drought months.

Druyan (1987, 1988) found that, in GCM simulations, ambient humidities were always lower over the Sahel during summer months that experienced less rainfall than other rainier model months. A survey of the literature leads to the conclusion that some Sahel droughts are related to deficiencies in the moisture supply while others may be the consequence of too few rain-generating wave disturbances (even when moisture is ample) (Druyan 1989).

In researching the low-moisture type of Sahel drought, it would be informative to determine the relative contributions to Sahel rainfall of atmospheric water vapor from different source regions. In light of the ambiguities raised by the research outlined above, one would like to know how and where interruptions to the moisture supply occur to induce precipitation deficiencies over the Sahel.

Corresponding author address: Dr. Leonard M. Druyan, NASA Goddard Space Flight Center, Goddard Institute for Space Studies, 2880 Broadway, New York, NY 10025.

2. GCM simulation studies

We present the results of two June–July simulations made with Climate Model II of the Goddard Institute for Space Studies (GISS) (Hansen et al. 1983). These simulations used the same prescribed climatological sea surface temperatures but were initialized on 1 June with different model atmospheric and land surface conditions. In both cases the initial conditions were taken from archived model histories. The model's horizontal grid resolution is 8° × 10°. The model climatology was previously shown to give a realistic representation of the African summer monsoon (Druyan 1987) and to be a useful tool for studying the climate dynamics of Sahel drought.

The two simulations produced significantly different precipitation rates over the Sahel. In June, the simulation that we call "rainy" produced higher rates over much of the sub-Sahara between 5°W and 20°E and over tropical Africa as well, with a maximum excess over the "dry" simulation of 8 mm day^{-1} at 12°N,10°E (Figs. 1a, b). The July precipitation fields (Figs. 1c and 1d) are similar to the corresponding June fields; in July, however, the maximum precipitation in the rainy simulation spread to the north and west. Over the western two-thirds of the sub-Sahara (8°–24°N, 15°W–25°E), the July accumulations in the rainy simulation averaged 93 mm, while the corresponding amount in the dry simulation was only 30 mm.

Our analysis focuses on the July precipitation differences in order to highlight the differential mechanisms that were operating during June and July. As stated, the two simulations differ with respect to atmospheric and land conditions over the entire global domain, and these differences include contrasting solutions for simulated June and July rainfall. We discuss the circulation characteristics that are relevant to the simulation of rainfall over the sub-Sahara, but the relationships between the African systems and the general circulation are not specifically addressed.

a. *Differences in atmospheric circulation*

Figure 2 shows the sea-level pressure distributions for the two simulations for June and July. Note the

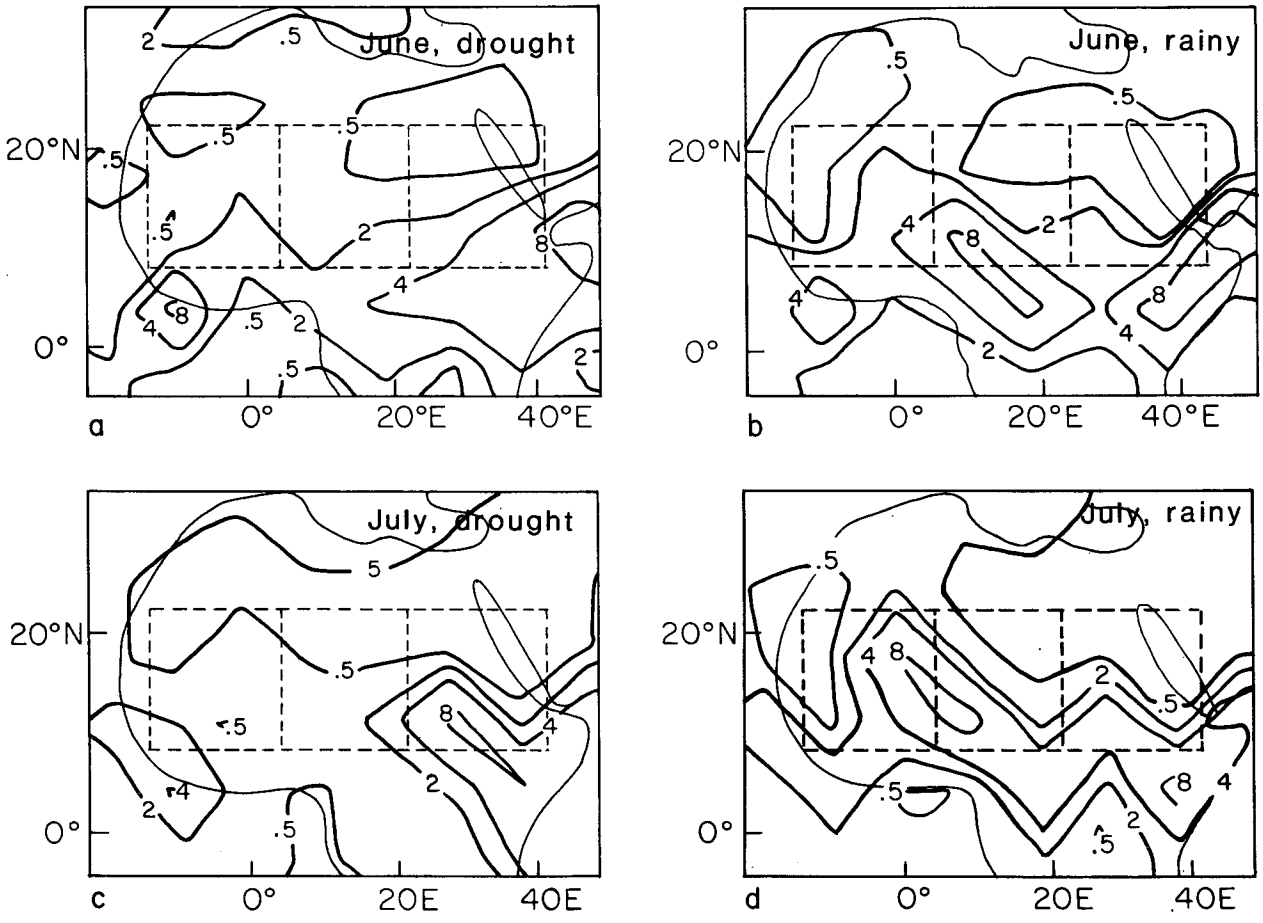

FIG. 1. Simulated precipitation distributions (mm day^{-1}): (a) drought simulation for June, (b) rainy simulation for June, (c) drought simulation for July, and (d) rainy simulation for July.

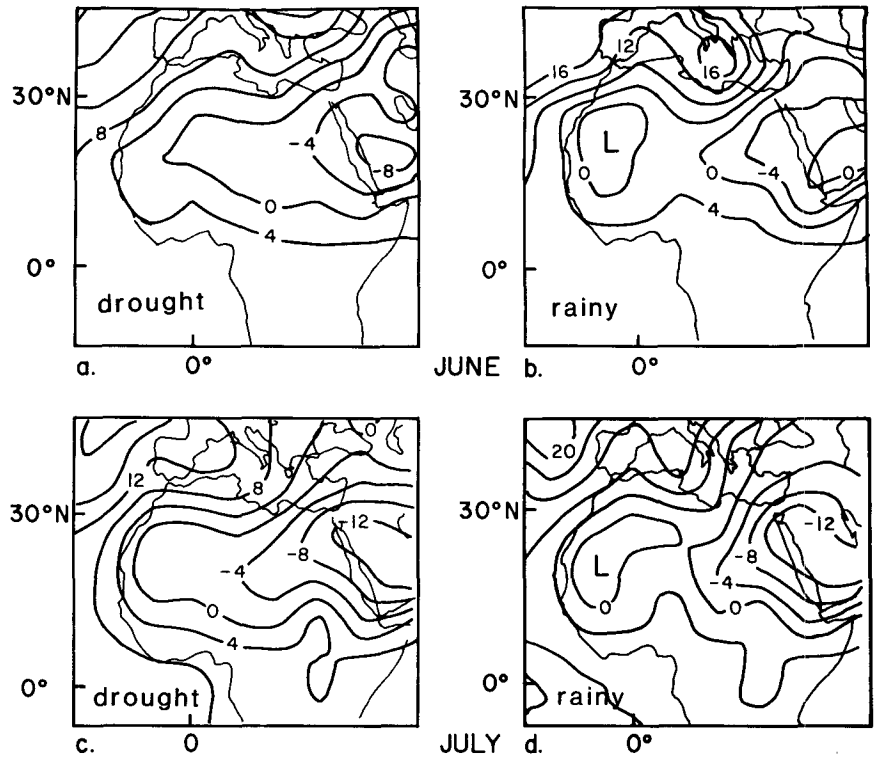

FIG. 2. Mean sea-level pressure distributions: (a) drought simulation for June, (b) rainy simulation for June, (c) drought simulation for July and (d) rainy simulation for July. (Isobars are labeled in mb-1000.)

closed low over the western Sahel in the rainy case for both months. In the drought case, a broad and shallower low pressure trough is maintained, bounded by steeper gradients to the north and south. Figure 3 shows the July mean zonal and meridional components of the computed winds interpolated to 900 mb from the model's two lowermost layers. The larger meridional pressure gradient along the southern boundary of the Sahel in the dry case is reflected by stronger zonal winds along 8°N that increase eastward from 15°W–15°E, promoting the divergence of moisture from the western Sahel. The rainy simulation features decreasing zonal winds along 8°N from 5°W to 25°E, and the closed low has initiated a meridional flow of about 4 m s^{-1} along 5°E (which does not appear in the second simulation) that advects moisture northward.

Figure 4 shows the July circulation at 200 mb and areas of convergence maxima and minima over northern Africa based on the resultant winds at that model level. In the rainy simulation, the axis of anticyclonic directional shear is aligned along 12°N, and the wind direction over the southern fringe of the Sahel is mostly easterly with areas of divergence from 0°–30°E at several latitudes over northern Africa; this may enhance moist convection by supporting ascending motion. The circulation over the drought conditions, however, indicates convergence at 200 mb along 0° in association with a trough in the westerlies that may suppress convective activity; divergence is confined to 30°–40°E. In this simulation, west of 20°E over Africa, easterly flow at 200 mb appears only along the equator.

b. Differences in ground wetness

In both simulations, the model's rainfall over the sub-Sahara is derived from water vapor that evaporated from a number of sources. The relative impact of continental evaporation on local rainfall in each simulation may be related to the *ground wetness*—the percent of saturation in the interactive soil moisture reservoir. While the average June ground wetness of the western Sahel was equal in the two runs, the June means for the central Sahel were 3.5% and 11.5% for the dry and rainy simulations, respectively, reflecting the differences in June precipitation rates (Fig. 1). The higher degree of ground saturation in the central Sahel probably enhanced the precipitation there in the rainy simulation.

3. Tracer results

The model runs incorporated a diagnostic method originally developed by Jouzel et al. (1987) for water isotopes. Following Koster et al. (1986, 1988), we have used the diagnostic here to trace water evaporating from selected source regions through the atmosphere in order to determine where this water precipitates. (A

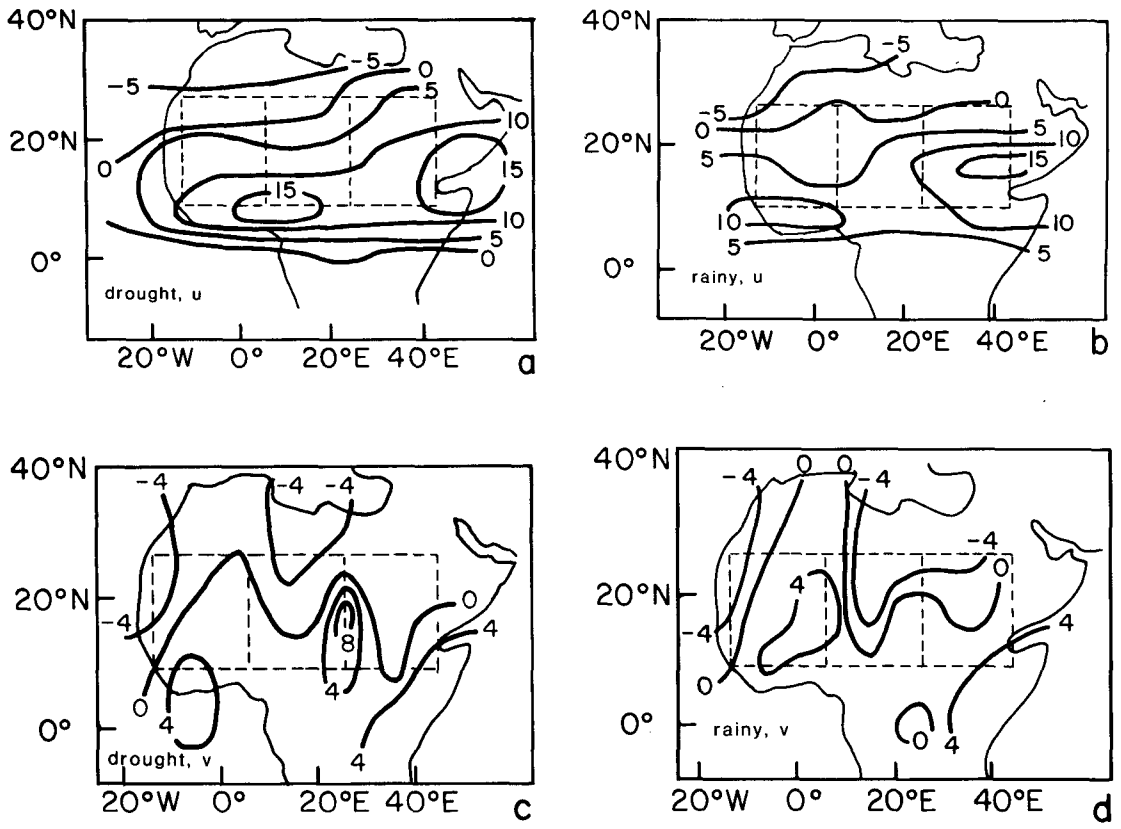

FIG. 3. July mean components of model winds at 900 mb (m s^{-1}): (a) zonal wind for drought simulation, (b) zonal wind for rainy simulation, (c) meridional wind for drought simulation, and (d) meridional wind for rainy simulation.

similar tracer diagnostic was employed by Joussaume et al. 1986, to examine the origins of continental precipitation in the GCM of the Laboratoire de Meteorologie Dynamique, Paris.) Figure 5 shows the location of nine source regions defined for this study, corresponding to water tracers 2 through 10. The remainder of the globe was defined as a tenth source region, designated as water tracer 11.

The relative contributions of each water tracer to the July precipitation over northern Africa are shown in Fig. 6 for the two simulations. The data are presented for three subdivisions of the sub-Sahara, corresponding to source regions 5, 6 and 7 in Fig. 5 and referred to below as the western Sahel, central Sahel and eastern Sahel, respectively. The water vapor present in the atmosphere at the beginning of the simulation was defined as water tracer 1. Figure 6 shows that its contribution to the July precipitation was small, indicating that most of the initial water vapor rained out in June.

Table 1 shows the evaporation computed for each of the source regions for June and July for both simulations. Note that evaporation amounts are not consistently lower for the drought case, although they are lower over the Atlantic Ocean in June and over the western two-thirds of the Sahel in July.

a. Western Sahel

Figure 6 shows that the tropical North Atlantic Ocean (area 4) contributes the most to rainfall in the western Sahel. Twice as much rain was realized from this source in the rainy simulation as in the drought case. Figure 7 suggests that in the drought run, more of the moisture from this source was advected to the eastern Sahel before it precipitated.

The circulation differences described above are consistent with the buildup and subsequent precipitation of more Atlantic Ocean water vapor over the western Sahel for the rainy case, and the more efficient eastward advection of moisture from the same source in the drought run. The closed low over the western Sahel has induced a strong low-level southerly flow that brings moisture northward to an area of very light westerlies in the rainy simulation (Fig. 3). In the drought simulation the flow is more zonal and stronger westerlies along 8°N direct this moisture eastward.

The second largest contribution to July rainfall over the western Sahel in both simulations was from local evaporation (Fig. 6). This contribution was five times larger in the rainy simulation, reflecting the greater evaporation rates in July (see Table 1). The greater

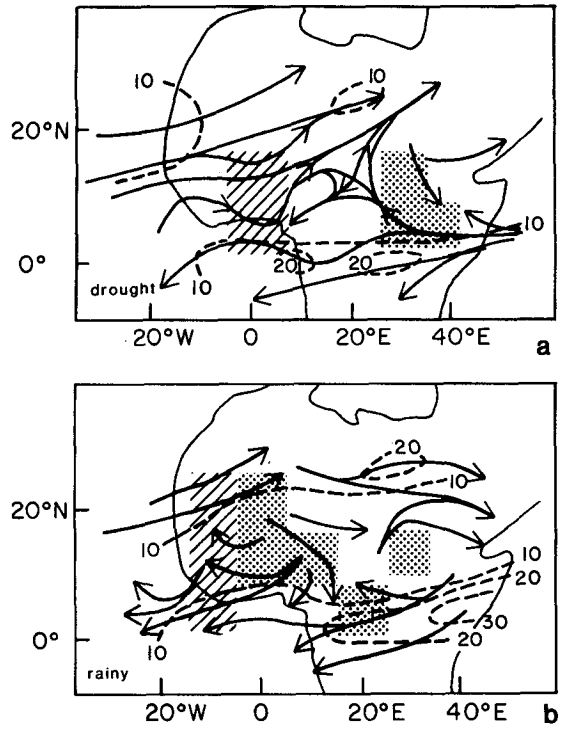

FIG. 4. Streamflow and isotachs based on 200 mb resultant winds for July: (a) drought simulation and (b) rainy simulation. Shaded areas indicate divergence and cross-hatched areas indicate convergence at 200 mb. (Isotachs labeled in m s^{-1}.)

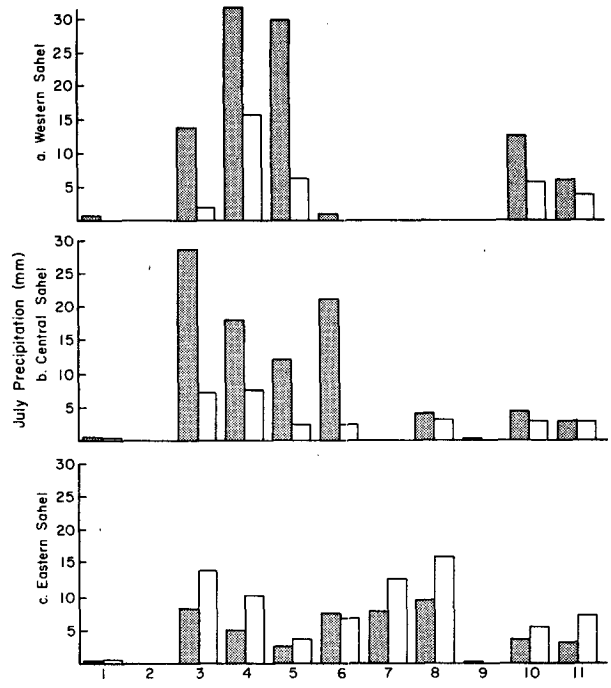

FIG. 6. Contributions to the July precipitation over three parts of the sub-Sahara for the simulations referred to as "rainy" (shaded) and "dry" (unshaded) in the text. The contributions are defined according to their evaporative sources, which are indicated along the horizontal axis. See Fig. 5 for the locations of these regions. (a) Over western Sahel (area 5), (b) over central Sahel (area 6), (c) over eastern Sahel (area 7).

evaporation, in turn, was a consequence of higher soil moisture (in July, but not in June) caused by more frequent episodes of precipitation. This supports the notion that ground moisture is a factor in Sahel seasonal precipitation totals (Nicholson 1988), although we must acknowledge that the initiation of this positive feedback requires that other factors be favorable for

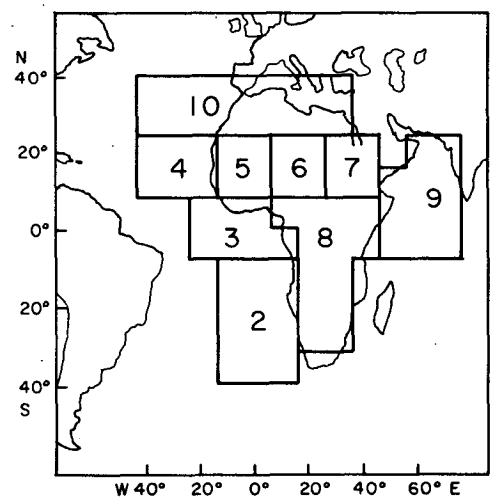

FIG. 5. The source regions for evaporation. Tracer number 1 was the moisture that was already ambient on 1 June, so it is not designated. Tracer 11 was the moisture evaporated from the domain not covered by source regions 2–10. Area 5 (western Sahel), area 6 (central Sahel) and area 7 (eastern Sahel) are comprised of four computational grid boxes each.

TABLE 1. Evaporation computed for each source region (mm) for rainy and drought simulations. Numbers correspond to labels in Fig. 5.

	June		July	
Source region	Rainy	Drought	Rainy	Drought
2 Eastern South Atlantic Ocean	186	175	152	155
3 Gulf of Guinea	180	168	148	160
4 Tropical North Atlantic Ocean	176	150	184	178
5 Western Sahel	40	46	72	34
6 Central Sahel	66	31	62	29
7 Eastern Sahel	35	85	60	79
8 Southern Africa	119	108	91	88
9 Western Indian Ocean	268	286	253	250
10 North Atlantic, Mediterranean, North Africa	107	83	91	95

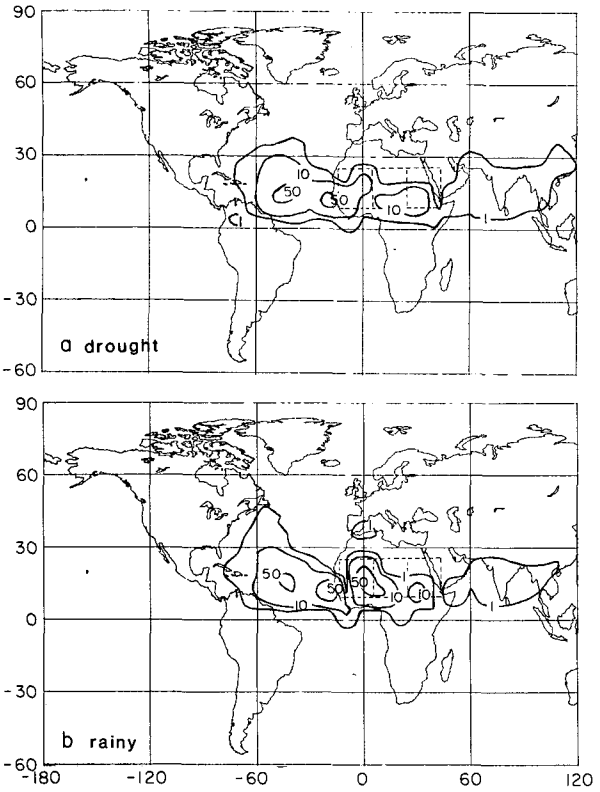

FIG. 7. The distribution of July precipitation derived from area 4 (see Fig. 5) evaporate: (a) drought simulation and (b) rainy simulation. The three Sahel areas discussed in the text are outlined. (Isopleths are labeled in mm.)

rainfall in the first place. Figure 8 shows, moreover, that in the drought run, the eastward moisture advection recalled above also deprived the western Sahel of some local evaporate, preferring to precipitate it farther to the east.

In contrast to the drought simulation, the calculation of western Sahel rainfall in the rainy case includes considerable moisture that evaporated from the Gulf of Guinea (area 3). We note that similar quantities of moisture evaporated from this source region in both simulations, but the drought version precipitated more of it locally near the coast of West Africa (Fig. 9), and immediately east of the source region near Brazil, as well as over the more distant east—the Persian Gulf and southwestern India. In the rainy case, the stronger southerly circulation near the prime meridian kept more of this moisture over the western third of the Sahel.

Figure 10 shows gains in precipitable water that result from the horizontal convergence of moisture from all sources. The atmosphere over the western Sahel gained about 26 mm of precipitable water during July in the rainy case, but only about 5 mm in the simulated drought as a result of differences in the local atmospheric circulation.

b. Central Sahel

In the rainy simulation, evaporate from the Gulf of Guinea (area 3) represents the most important source of moisture for precipitation over the central Sahel. In the drought case, however, only 25% as much Gulf of Guinea water precipitated there, and much less rainfall was derived from tropical North Atlantic (area 4) moisture as well. The reasons for these differences parallel those cited above for the western Sahel.

Table 1 shows that the evaporation from the central Sahel was about twice as great in the rainy case during both months, and Fig. 6 shows that this local evaporation was a large component of the precipitation there. This supports the idea that much of the difference in the July rainfall over the central Sahel (Fig. 6) in this study can be explained by the differential wetting of the ground there in June (recalled above). A similar analysis applies also to the northeast grid box of the western Sahel, but not to the western Sahel as a whole.

Figure 6 shows that continental evaporation from the western and central Sahel accounted for six times as much precipitation over the central Sahel in the rainy simulation as in the dry simulation. On the other hand, the total local evaporation from these continental sources was only twice as great in the rainy case in July and less than twice in June. Thus, the difference in central Sahel precipitation derived from local and

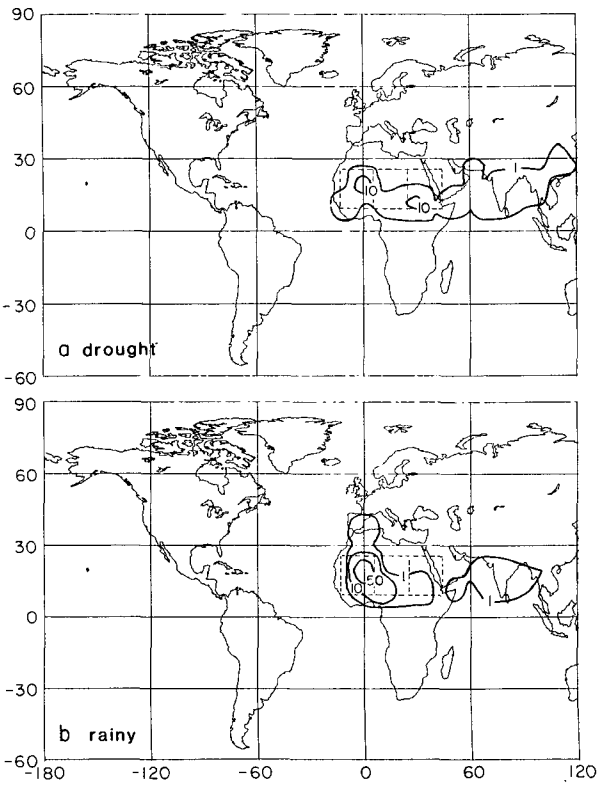

FIG. 8. As in Fig. 7, but for area 5.

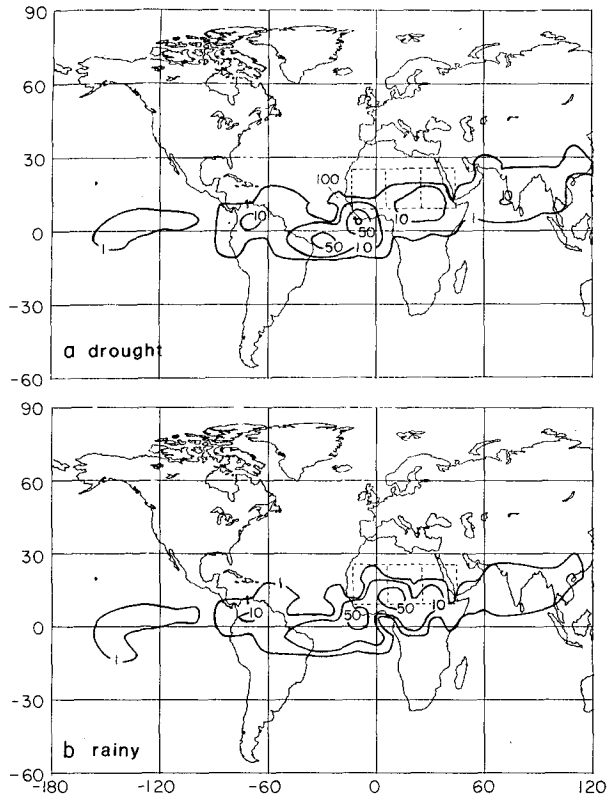

FIG. 9. As in Fig. 7, but for area 3.

nearby continental evaporation was more extreme than the difference in the potential water supply from the amounts that evaporated. By comparing the areas enclosed by the 1 mm contours in Fig. 8, one can discern that a larger proportion of the water vapor from the western Sahel was advected toward Asia in the drought simulation, apparently by stronger westerly winds. Similarly, Fig. 11 shows that very little of the evaporate from the central Sahel precipitated locally in the drought case, much having been carried eastward.

Figure 10 shows that horizontal moisture convergence over the central Sahel was greater for the rainy experiment, with 26 mm gained, than for the dry case where only 7 mm of precipitable water was added.

c. *Eastern Sahel*

More July precipitation was calculated for the eastern Sahel (area 7) in the simulation we called "drought" as a result of greater moisture convergence from the Atlantic Ocean and more local evaporation. Similar amounts of water vapor from the western and central Sahel precipitated here in both simulations. Figure 10 clearly shows a maximum convergence of moisture in the drought simulation, for which an average of about 13 mm of precipitable water was added to the atmosphere over the eastern Sahel; in the rainy case, about 9 mm was lost by horizontal divergence.

The link between the precipitation over northeast Africa and Indian Ocean sea-surface temperatures (SST) has been a matter of speculation. Palmer (1986) and Bhatt (1989) have found indirect evidence associating eastern Sahel rainfall with Indian Ocean SST. Cadet and Nnoli (1987) show that considerable moisture is advected from the east at midtropospheric levels over northern Africa, but this flux does not provide moisture convergence over the Sahel, so it cannot contribute to the rainfall there. Moreover, Cadet and Nnoli conclude that this moisture originates over Africa since they found little advection of moist air from the Indian Ocean after mid-June. Area 9 in Fig. 5 is the area of the western Indian Ocean from which evaporated water was traced in the present study. Almost none of this moisture precipitated over any of the Sahel in either run; all of the rainfall from this source consistently remained east of 40°E, supporting the conclusions of Cadet and Nnoli. Of course, this does not preclude other influences that Indian Ocean SST may have on Sahel rainfall via modifications of low-level circulation characteristics.

4. Discussion

The GCM simulations discussed in the present study focus on July Sahel precipitation. Of course, July is

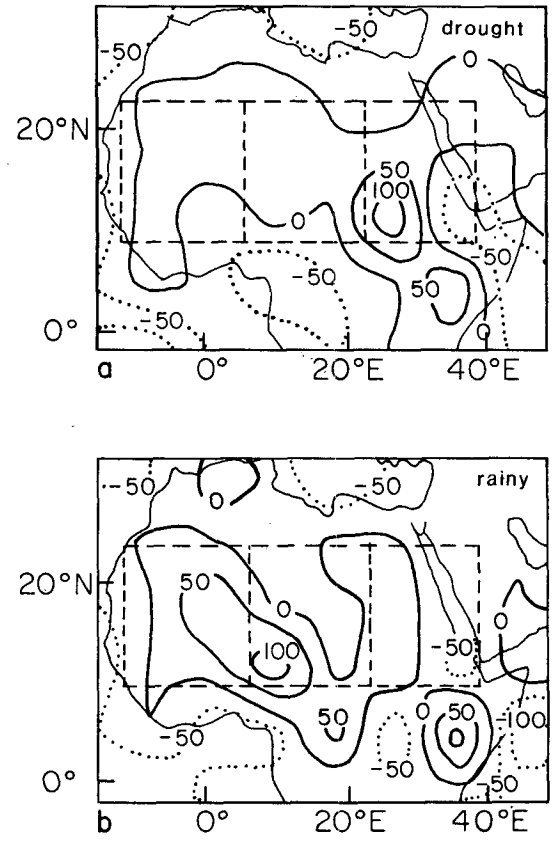

FIG. 10. Gains in precipitable water (mm) for July resulting from the horizontal convergence of moisture from all sources: (a) drought simulation and (b) rainy simulation.

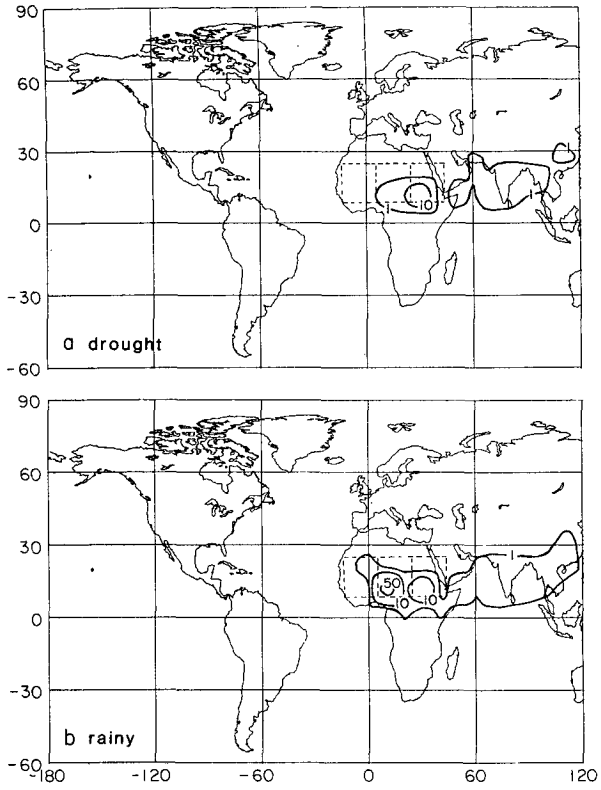

FIG. 11. As in Fig. 7, but for area 6.

only one rainy month during the summer monsoon season. While the mechanisms documented here are probably valid explanations of some anomalous seasonal rainfalls, we recognize that each month need not be the same as the preceding or following month and that a wide variety of scenarios is certainly possible. Moreover, since the analysis is based on a simulation model that only approximates real climatic processes, certain details of the results probably differ from actual atmospheric behavior. For example, the model does not resolve the wave disturbances or their associated squall lines that trigger most of the sub-Saharan rainfall. Instead, a moist convection parameterization that uses the temperature and humidity profiles of the gridpoint data determines rainfall rates as a proxy for the actual events within mesoscale convective towers. These profiles are influenced by computations of diabatic processes, ground hydrology and the simulated circulation with its associated horizontal and vertical transports of heat and moisture.

One of the most interesting findings of these tracer studies is that model drought in the Sahel can occur even when evaporation from the tropical North Atlantic and Gulf of Guinea is not anomalous and even when the resulting water vapor fluxes into the western Sahel are not deficient. In the present experiments, model drought was a consequence of weak moisture convergence caused by a shallow monsoon trough over the western Sahel. Although moisture flux was not inhibited from the ocean sources, water vapor drifted eastward without building up humidities over the western and central Sahel sufficiently for efficient rainfall. This offers a reasonable explanation of Lamb's (1983) computation of high flux along the Gulf of Guinea coast during several dry seasons. We found that the Sahel was also deprived of some Gulf of Guinea moisture in the drought case by additional precipitation (of this moisture) near the coasts of West Africa and South America as well as far downwind over India.

There was evidence that heavy Sahel rainfall during June and early July provided moisture for later precipitation through the recycling of local evaporation. For example, some of the differences in July evaporation rates reflected the relative values of ground wetness that developed during the second month. In the rainy simulation the average ground wetness for the entire sub-Sahara nearly doubled between June and July. In the dry simulation, however, decreases in ground wetness over the western and central Sahel were consistent with smaller contributions of local evaporate to lower rainfall rates. Nevertheless, most of the differences in rainfall between the drought and rainy simulations are attributable to dissimilar July circulations that gave rise to different trajectories of evaporate from nonlocal sources—mostly from the oceans, but also from adjacent continental areas.

Indian Ocean evaporate did not precipitate at all over the Sahel, consistent with the observational evidence of Cadet and Nnoli (1987). The links implied by other studies between Indian Ocean SST and Ethiopian rainfall may reflect changes in circulation that favor or inhibit moisture convergence over the Eastern Sahel. For example, a weakening of the Indian Ocean monsoon circulation associated with warm Arabian Sea SST could in turn weaken fluxes from the southwest that supply moisture to northeastern Africa. In the present study, these circulation and moisture advection differences developed as a result of other influences.

The contrasting circulation patterns that accounted for the important differences in moisture convergence evolved from the different 1 June initial conditions, which were taken from two archived model histories. The June–July circulation in each case was undoubtedly influenced by a prior atmospheric evolution that is not addressed by this study. However, it may be significant that the evaporation from the combined Atlantic Ocean source regions was lower for the drought case in June. Thus, lower moisture fluxes during the early summer, leading to less latent heat release over West Africa, may have slowed the deepening of the pressure trough during June and July, consequently encouraging the eastward advection of moisture away from the western and central Sahel. These hypotheses can be tested by longer simulations with water tracer diagnostics.

5. Conclusion

We present an analysis of two June–July simulations of the GISS climate model that produced markedly different precipitation rates over the sub-Sahara in July. For both the "drought" and "rainy" simulations, diagnostic procedures incorporated into the model provided the components of the precipitation derived from each of ten source regions of evaporation.

The model results indicate the importance of recycling continental evaporate, but suggest that water from the Indian Ocean does not precipitate over the sub-Sahara. The differences in Sahelian precipitation rates were primarily a consequence of the contrasting circulations. Although July evaporation from the relevant oceanic sources was approximately the same for the two simulations, atmospheric circulation favored convergence of this moisture over the western Sahel in one case, and over the eastern Sahel in the other case.

Acknowledgments. We wish to thank Dr. David Rind for suggesting the study and for reviewing the manuscript. R. Suozzo assisted in the data processing.

REFERENCES

Bhatt, U., 1989: On circulation regimes of drought in the African-South Asian monsoon belt. *J. Climate,* **2,** 1133–1144.

Cadet, D., and N. Nnoli, 1987: Water vapour transport over Africa and the Atlantic Ocean during summer 1979. *Quart. J. Roy. Meteor. Soc.,* **113,** 581–602.

Druyan, L., 1987: GCM studies of the African summer monsoon. *Clim. Dyn.,* **2,** 117–126.

——, 1988: SST/Sahel drought teleconnections in GCM simulations. *Recent Climatic Change-a Regional Approach,* S. Gregory, Ed., Belhaven Press, 154–165.

——, 1989: Advances in the study of sub-Saharan drought. *Int. J. Climatol.,* **9,** 77–90.

Hansen, J., G. Russell, D. Rind, P. Stone, A. Lacis, S. Lebedeff, R. Ruedy and L. Travis, 1983: Efficient three-dimensional global models for climate studies: Models I and II. *Mon. Wea. Rev.,* **111,** 609–662.

Joussaume, S., R. Sadourny and C. Vignal, 1986: Origin of precipitating water in a numerical simulation of the July climate. *Ocean-Air Interactions,* **1,** 43–56.

Jouzel, J., G. Russell, R. Suozzo, R. Koster, J. White and W. Broecker, 1987: Simulations of the HDO and $H_2{}^{18}O$ atmospheric cycles using the NASA GISS general circulation model: The seasonal cycle for present-day conditions. *J. Geophys. Res.,* **92,** 14 739–14 760.

Koster, R., J. Jouzel, R. Suozzo, G. Russell, W. Broecker, D. Rind and P. Eagleson, 1986: Global sources of local precipitation as determined by the NASA/GISS GCM. *Geophys. Res. Lett.,* **13,** 121–124.

——, P. Eagleson and W. Broecker, 1988: Tracer water transport and subgrid precipitation variation within atmospheric general circulation models. *Tech. Rep. 317,* 364 p. [Available from Dept. of Civil Engineering, MIT, Cambridge, MA.]

Lamb, P., 1983: West African water vapor variations between recent contrasting Subsaharan rainy seasons. *Tellus,* **35A,** 198–212.

Nicholson, S., 1988: Land surface atmosphere interaction: Physical processes and surface changes and their impact, *Progr. Phys. Geogr.,* **12,** 36–65.

Palmer, T., 1986: Influence of the Atlantic, Pacific and Indian Oceans on Sahel rainfall. *Nature,* **322,** 251–253.